# Vegetation Stress Detection through Chlorophyll $a + b$ Estimation and Fluorescence Effects on Hyperspectral Imagery

P. J. Zarco-Tejada,* J. R. Miller, G. H. Mohammed, T. L. Noland, and P. H. Sampson

## ABSTRACT

**Physical principles applied to remote sensing data are key to successfully quantifying vegetation physiological condition from the study of the light interaction with the canopy under observation. We used the fluorescence–reflectance–transmittance (FRT) and PROSPECT leaf models to simulate reflectance as a function of leaf biochemical and fluorescence variables. A series of laboratory measurements of spectral reflectance at leaf and canopy levels and a modeling study were conducted, demonstrating that effects of chlorophyll fluorescence (CF) can be detected by remote sensing. The coupled FRT and PROSPECT model enabled CF and chlorophyll $a + b$ ($C_{a+b}$) content to be estimated by inversion. Laboratory measurements of leaf reflectance ($r$) and transmittance ($t$) from leaves with constant $C_{a+b}$ allowed the study of CF effects on specific fluorescence-sensitive indices calculated in the Photosystem I (PS-I) and Photosystem II (PS-II) optical region, such as the curvature index [CUR; $(R_{675}{\cdot}R_{690})/R^2_{683}$]. Dark-adapted and steady-state fluorescence measurements, such as the ratio of variable to maximal fluorescence ($F_v/F_m$), steady state maximal fluorescence ($F'_m$), steady state fluorescence ($F_t$), and the effective quantum yield ($\Delta F/F'_m$) are accurately estimated by inverting the FRT–PROSPECT model. A double peak in the derivative reflectance (DR) was related to increased CF and $C_{a+b}$ concentration. These results were consistent with imagery collected with a compact airborne spectrographic imager (CASI) sensor from sites of sugar maple (*Acer saccharum* Marshall) of high and low stress conditions, showing a double peak on canopy derivative reflectance in the red-edge spectral region. We developed a derivative chlorophyll index (DCI; calculated as $D_{705}/D_{722}$), a function of the combined effects of CF and $C_{a+b}$ content, and used it to detect vegetation stress.**

Most current assessments of forest condition are limited to ground-based visual evaluation (e.g., Canadian Forest Service, 1999). Although these conventional field assessments are valuable, they do not reveal physiological changes that characterize early stress responses (Sampson et al., 2000). Assessing physiological condition can indicate productivity and adaptability to environmental stress (Chapin, 1991; Colombo and Parker, 1999) and may provide early indication of decline in stand vigor and productive capacity. Early detection of stress with remote sensing methods could help to identify stress status at larger temporal and spatial scales and before damage is visible. However, to determine vegetation condition from the study of the interaction between the light and the canopy under observation, physical methods must be developed (Zarco-Tejada, 2000).

The $C_{a+b}$ content is a potential indicator of vegetation stress because of its direct role in the photosynthetic processes of light harvesting and initiation of electron transport and its responsiveness to a range of stresses. In the chloroplast, light energy is harvested and processed by two functional units designated Photosystem I (containing chlorophyll with an absorption peak at 700 nm) and Photosystem II (chlorophyll absorption peak at 680 nm), which produce oxygen and energy through a series of reduction–oxidation reactions to transport electrons. Stressed vegetation can undergo various physiological perturbations in the light-dependent reactions of photosynthesis, including disruption of electron transfer, production of deleterious oxygen derivatives, photobleaching, pigment-bed reorganization, and structural damage to photosynthetic pigments. Differences in remote sensing reflectance between healthy and stressed vegetation due to changes in $C_{a+b}$ levels have been detected previously in the green peak and along the red-edge spectral region (690 to 750 nm) (e.g., Rock et al., 1988; Vogelmann et al., 1993; Carter, 1994; Gitelson and Merzlyak, 1996).

Assessing CF is also a well-established physiological approach to detect previsual strain (Mohammed et al., 1995). Changes in chlorophyll function often precede changes in chlorophyll content, hence CF changes are often observed long before leaves become chlorotic. Chlorophyll fluorescence is red and far-red light produced in photosynthetic tissues upon excitation with natural or artificial light in the visible spectrum. Chlorophyll fluorescence production is one way plant chloroplasts harmlessly dissipate light energy that exceeds photosynthesis requirements, thereby protecting the chloroplasts from light-induced oxidative damage. According to several reviews of CF theory, measurement methods and interpretation (e.g., Papageorgiou, 1975; Krause and Weis, 1984; Schreiber and Bilger, 1987; Lichtenthaler and Rinderle, 1988; Lichtenthaler, 1992; Larcher, 1994; Schreiber et al., 1994), steady state CF and photosynthetic rate are inversely related (i.e., CF is low when photosynthesis is high). In addition, CF techniques

P.J. Zarco-Tejada, Centre for Research in Earth and Space Science (CRESS), and J.R. Miller, Dep. of Physics and Astronomy, York University, 4700 Keele Street, Toronto, ON, Canada M3J 1P3. G.H. Mohammed, P&M Technologies, 66 Millwood St., Sault Ste. Marie, ON, Canada P6A 6S7. T.L. Noland, Ontario Forest Research Institute (OFRI), Ontario Ministry of Natural Resources (OMNR), Sault Ste. Marie, ON, Canada P6A 2E5. P.H. Sampson, Provincial Geomatics Service Centre, Ontario Ministry of Natural Resources, 300 Water St, Peterborough, ON, Canada K9J 8M5. Received 24 Jan. 2001. *Corresponding author (zarco@terra.phys.yorku.ca).

Published in J. Environ. Qual. 31:1433–1441 (2002).

**Abbreviations:** CASI, compact airborne spectrographic imager; CF, chlorophyll fluorescence; $C_{a+b}$, chlorophyll $a + b$; CUR, reflectance curvature index $[(R_{675}{\cdot}R_{690})/R^2_{683}]$; DCI, derivative chlorophyll index; $D_x$, value of the derivative reflectance at wavelength $X$ in nanometers; FRT, fluorescence–reflectance–transmittance model; $F'_m$, steady state maximal fluorescence; $F_t$, steady state fluorescence; $F_v/F_m$, ratio of variable to maximal fluorescence; $\Delta F/F'_m$, effective quantum yield; PAM, pulse amplitude modulation; PS-I, Photosystem I; PS-II, Photosystem II; RMSE, root mean square error; RT, radiative transfer; $R_x$, value of the reflectance at wavelength $X$ in nanometers.

are rapid, nondestructive, and noninvasive (Mohammed et al., 1995).

Evidence of a solar-induced fluorescence signal superimposed on leaf reflectance signatures was first reported by Buschmann and Lichtenthaler (1988) as a result of laboratory studies with a reflection–absorption–fluorescence spectrometer. Other studies of the effect of fluorescence in apparent reflectance have been conducted (Peñuelas et al., 1995; Gamon et al., 1997; Peñuelas et al., 1997, 1998; Gamon and Surfus, 1999; Gitelson et al., 1999), although the effect of the fluorescence signal on the apparent reflectance spectra of leaves has not been quantified.

A study of whether chlorophyll fluorescence is measurable with a passive instrument such as an airborne hyperspectral imager (Zarco-Tejada, 2000) showed that radiative transfer (RT) theory, constrained by appropriate modeling assumptions, can be investigated at leaf, laboratory, and near-field scales to demonstrate that CF effects are detectable as part of leaf reflectance and transmittance, as well as near-canopy reflectance measurements collected over vegetation. Further studies of the theoretical basis for quantitatively estimating pigments by scaling up optical indices have focused on remote sensing methods based on RT and infinite reflectance models (Zarco-Tejada et al., 2000a,b, 2001a,b).

Extensive research performed at the leaf level have demonstrated the use of a large number of optical indices for $C_{a+b}$ estimation, enabling the study of differences in reflectance between healthy and stressed vegetation due to changes in pigment levels (e.g., Rock et al., 1988; Vogelmann et al., 1993; Carter, 1994). Estimating pigment content with optical indices has been shown to produce the best results at leaf and canopy levels with red-edge, spectral, and derivative red-edge indices (Zarco-Tejada et al., 2001b).

Investigation of the effects of fluorescence contributions to the remotely observed signature identified optical indices calculated from leaf reflectance measurements related specifically to fluorescence emission in the 680- to 740-nm spectral region due to PS-II and PS-I (Zarco-Tejada et al., 2000a,b). Indices related to fluorescence maxima at 685 and 735 nm may be useful to study the relationship of leaf and canopy reflectance with chlorophyll fluorescence, such as $R_{685}/R_{655}$, $R_{683}^2/(R_{675}\cdot R_{691})$, and $D_{730}/D_{706}$.

These indices were assessed through RT modeling with the FRT simulation model (Zarco-Tejada et al., 2000a), which includes fluorescence flux in the RT differential equations. Here we discuss the results of an assessment of a coupled FRT with the PROSPECT leaf model (Jacquemoud and Baret, 1990) for fluorescence estimation by model inversion. Further, we look at the effects of chlorophyll fluorescence and pigment content on the derivative reflectance, focusing on the understanding of such effects on hyperspectral imagery collected with the airborne CASI instrument.

## MATERIALS AND METHODS

### Data Collection

In 1998 and 1999, leaf material was sampled from three-year-old potted trees of sugar maple for laboratory–greenhouse experiments and from twelve 30- × 30-m sugar maple study sites in the Algoma Region, Ontario, Canada.

The greenhouse experiments required one set of 30 leaves with similar chlorophyll content (49 to 53 units according to SPAD-502 [Minolta Camera Co., Osaka, Japan] chlorophyll meter readings and from subsequent pigment analysis, $\bar{x}$ = 58.08 μg/cm$^2$, $s$ = 5.26, $n$ = 30). Leaf samples with similar chlorophyll content were required to study how the apparent leaf reflectance and transmittance vary due to the effects of chlorophyll fluorescence. For the second greenhouse experiment, 60 leaves with variable chlorophyll content ($\bar{x}$ = 35.66 μg/cm$^2$, $s$ = 15.87, $n$ = 60) were sampled to study variations in the apparent leaf reflectance and transmittance due to changes in pigment content and chlorophyll fluorescence and were used to estimate pigment by model inversion.

In 1998 and 1999, 440 single leaf samples were collected from the 12 sugar maple study sites. Reflectance and transmittance were measured on these leaf samples with a LI-COR (Lincoln, NE) 1800-12 integrating sphere, coupled by a 200-μm-diameter single mode fiber to an Ocean Optics (Dunedin, FL) Model ST 1000 spectrometer, with a 1024-element detector array, 0.5-nm sampling interval, and approximately 7.3-nm spectral resolution in the 340- to 860-nm range.

Chlorophyll fluorescence variables $F_v/F_m$, $F_t$, $\Delta F/F'_m$, and $F'_m$ were measured with a pulse amplitude modulation (PAM) fluorometer (PAM-2000; Heinz Walz GmbH, Effeltrich, Germany), which has been used widely in basic and applied fluorescence research (Mohammed et al., 1995). The term $F_v/F_m$ quantifies the maximal efficiency of photon capture by open PS-II reaction centers and is one of the most widely used chlorophyll fluorescence variables. It is calculated from the equation $F_v/F_m = (F_m - F_o)/F_m$, where $F_m$ is the maximal fluorescence yield of a dark-adapted sample, with all PS-II reaction centers fully closed, and $F_o$ is the minimum fluorescence yield of a dark-adapted sample, with all PS-II reaction centers fully open. Effective quantum yield, which denotes the actual efficiency of PS-II photon capture of light by closed PS-II reaction centers, was determined as $\Delta F/F'_m = (F'_m - F_t)/F'_m$, where $F'_m$ is the maximal fluorescence of a pre-illuminated sample with PS-II centers closed, and $F_t$ is the fluorescence at steady state. Procedures used for measuring $F_v/F_m$ and $\Delta F/F'_m$ were based on standard methods (Heinz-Walz-GmbH, 1993). To measure maximal fluorescence induction $F_v/F_m$, leaves were dark-adapted in bags at room temperature for at least 30 min.

In 1998 and 1999, airborne hyperspectral imagery was collected over the 12 sites of sugar maple where ground-truth samples were collected. The CASI sensor acquired hyperspectral reflectance data at 2-m spatial resolution and 72 spectral channels with 7.5-nm spectral bandwidth. The 12-bit radiometric resolution data collected by CASI were processed to at-sensor radiance with calibration coefficients derived in the laboratory. Simultaneously, a Micro-Tops II sunphotometer (Solar Light Co., Philadelphia, PA) was used to collect aerosol optical depth data at 550 nm so image data could be processed to ground reflectance with the CAM5S atmospheric correction model (O'Neill et al., 1997). Reflectance data were georeferenced with GPS data collected aboard the aircraft. Final registration of the hyperspectral mode imagery was achieved by registration to the CASI high spatial resolution imagery with visual identification of ground-referenced 1-m white targets, which served to accurately identify the location of the sites.

### Modeling Chlorophyll Fluorescence and Chlorophyll $a + b$ Estimates at the Leaf Level with the Fluorescence–Reflectance–Transmittance and PROSPECT Models

Chlorophyll fluorescence effects on apparent reflectance were simulated at leaf level to validate the coupled FRT–

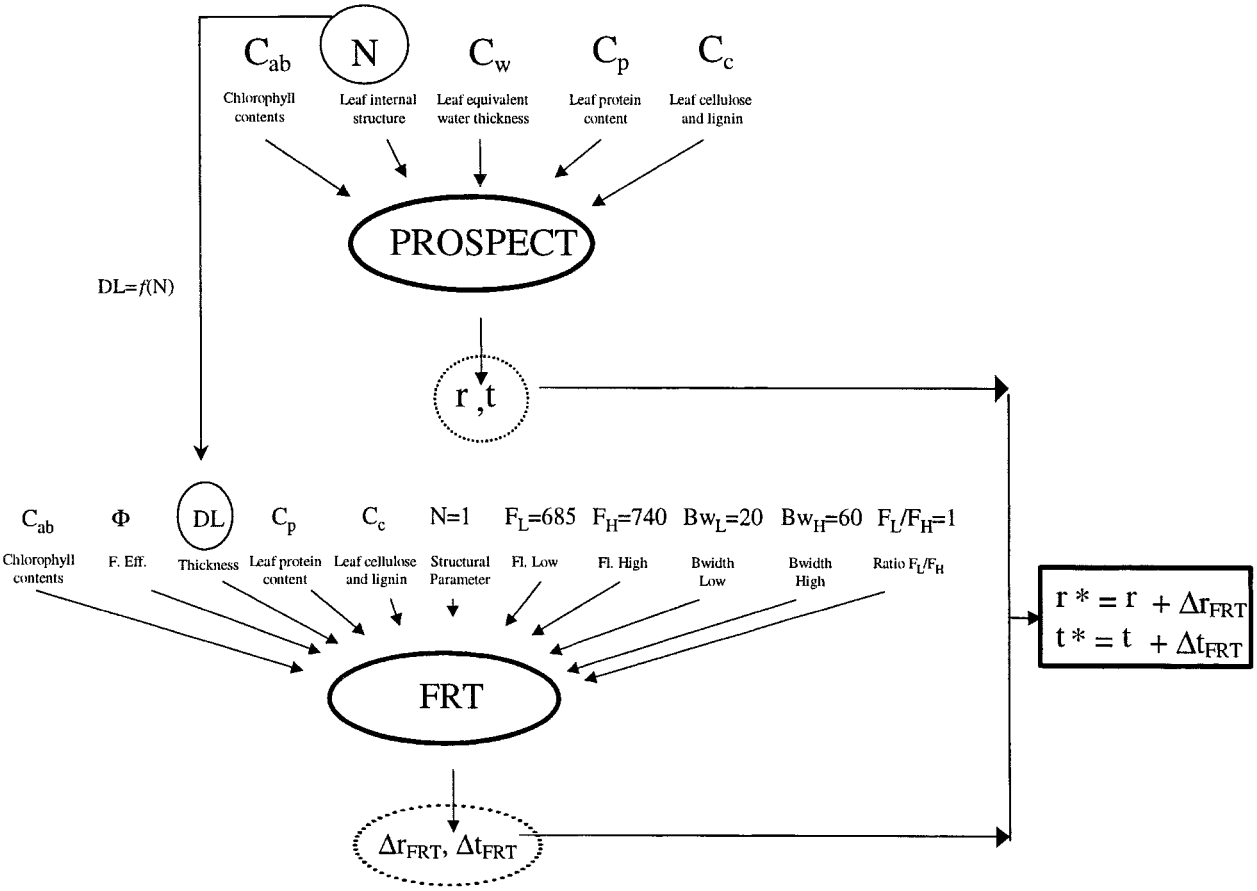


**Fig. 1. Schematic diagram showing the coupling between the fluorescence–reflectance–transmittance (FRT) and PROSPECT models to calculate the change in reflectance ($r^*$) and transmittance ($t^*$) caused by accounting for chlorophyll fluorescence.**

PROSPECT model (Fig. 1). The FRT model coupled to PROSPECT was used to simulate the effects of CF and variable $C_{a+b}$ concentration on the derivative of reflectance to understand spectral features observed from airborne hyperspectral reflectance images collected at 2- × 2-m spatial resolution from healthy and stressed sugar maple study sites.

Experimental leaf reflectance, transmittance, pigment content, and chlorophyll fluorescence data were used for assessments through inversion of the coupled model by iterative optimization. The CF effects on leaf reflectance were simulated with the FRT model with input parameters leaf thickness (DL), $C_{a+b}$ content ($\mu g/cm^2$), nominal values of protein content ($C_p$, in $g/cm^2$), cellulose and lignin content ($C_c$, in $\mu g/cm^2$), and equivalent water thickness ($C_w$, in cm). The fluorescence signal simulation inputs were the photon fluorescence efficiency ($\phi$), ratio $f$ ($F_L/F_H$) of the fluorescence peak at $F_L$ (P-II center wavelength) relative to that at $F_H$ (P-I center wavelength), and bandwidths $B_L$ and $B_H$, the full width at half maximum of the fluorescence emissions centered at $F_L$ and $F_H$ wavelengths, respectively.

The coupling method consisted of adding the fluorescence signal modeled by FRT to the leaf reflectance and transmittance spectra simulated by PROSPECT, linking the variables DL (from FRT model) and the structural parameter ($N$) of the leaf mesophile (dimensionless, from PROSPECT model) through an empirical relationship. The rest of the input parameters needed in FRT for fluorescence modeling ($F_L$, $B_L$, $F_H$, $B_H$, $f$, and $\phi$) allowed calculation of fluorescence spectra in the 400- to 800-nm range, $\Delta r_{FRT}$ and $\Delta t_{FRT}$, obtaining the final apparent reflectance ($r^*$) and transmittance ($t^*$) as $r^* = r + \Delta r_{FRT}$; $t^* = t + \Delta t_{FRT}$ (Fig. 2).

Canopy reflectance without the effects of fluorescence was simulated with the SAILH canopy reflectance model (Verhoef, 1984) with simulated leaf reflectance and transmittance from PROSPECT.

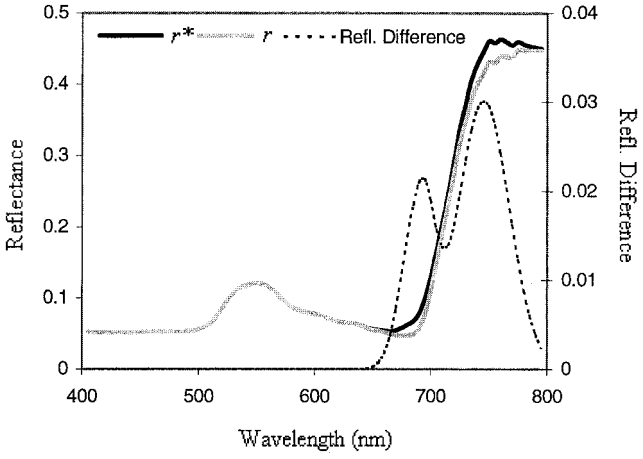


**Fig. 2. Fluorescence–reflectance–transmittance (FRT) model simulation of leaf reflectance with the effects of fluorescence flux. Parameters used for the simulation: $\phi$ = 0.085, $C_{a+b}$ content = 50 $\mu g/cm^2$, $D_L$ = 0.075 mm, $F_L$ = 688 nm, $B_L$ = 30 nm, $F_H$ = 746 nm, $B_H$ = 52 nm, $f$ ratio $F_H/F_L$ = 0.94, labeled as $r^*$ (with fluorescence), $r$ (without fluorescence).**

The FRT–PROSPECT model for estimating leaf $C_{a+b}$ was assessed with greenhouse experiment data on 60 leaves with variable chlorophyll content and fluorescence. The model was inverted by iterative optimization, varying the structural parameter $N$ from 0.9 to 1.6 to minimize the root mean square error (RMSE) function $\xi(N)$ (Eq. [1]) with both reflectance and transmittance in the near infrared NIR (780–800 nm), where structural effects are dominant in reflectance and transmittance:

$$\text{RMSE} = \xi(N, C_{a+b}) = \sqrt{\frac{\sum_{\lambda} [(r - r_m)_{\lambda}^2 + (t - t_m)_{\lambda}^2]}{n}} \quad [1]$$

where $r_m$ and $t_m$ are reflectance and transmittance measured from the leaf samples with the LI-COR 1800-12 integrating sphere coupled to the fiber spectrometer, and $r$ and $t$ are reflectance and transmittance simulated by the PROSPECT model. In the second step, with $N$ estimated, $C_{a+b}$ was varied from 10 to 70 μg/cm$^2$ and the function $\xi(N, C_{a+b})$ minimized by calculating the RMSE for the 450- to 700-nm range.

The coupled PROSPECT and FRT model for fluorescence estimation was assessed by looking at the spectral region where CF affects apparent reflectance. The CUR curvature index $[(R_{675}\cdot R_{690})/R_{683}^2]$, which was found to correlate strongly with fluorescence (Zarco-Tejada et al., 2000a,b), was used for this assessment. The CUR calculated by the coupled FRT–PROSPECT model in the forward direction was compared with the CUR measured from leaf reflectance samples with variable CF and constant and variable $C_{a+b}$ contents. Input parameters were $C_{a+b}$ measured from the single leaves and $N$ estimated by inverting the PROSPECT model with experimental reflectance and transmittance data. For FRT simulation, inputs were $F_L$, $B_L$, $F_H$, $B_H$, and fluorescence efficiency $\phi$ set to 0 (to simulate the CUR without fluorescence effects), and set to PAM-measured variables $F_v/F_m$, $F'_m$, and $\Delta F/F'_m$ (to simulate the CUR with fluorescence effects). Steady state fluorescence variables were measured with a halogen light attachment (excitation wavelength < 710 nm) at 110 and 2820 μmol quanta/(m$^2$ s) to correspond to photosynthetic photon flux densities used to measure reflectance and transmittance with the LI-COR sphere (indicated hereafter as $\Delta F/F'_m110$, $F'_m110$, $\Delta F/F'_m2820$).

### Detecting Stress by Modeling the Effects of Chlorophyll *a* + *b* and Chlorophyll Fluorescence at the Canopy Level with Hyperspectral Data

The effects of chlorophyll fluorescence on apparent reflectance and derivative reflectance were modeled with the FRT–PROSPECT RT model. Simulated fluorescence spectra were modeled with FRT using $\phi = 0.1$, 0.15, and 0.2, fluorescence emission centers at 695 nm ($B_L$ = 30 nm bandwidth) and 750 nm ($B_H$ = 40 nm), leaf structural parameter $N$ = 1.5, and $C_{a+b}$ = 40 μg/cm$^2$ (Fig. 3, top left). These were added to leaf reflectance simulated by the PROSPECT model (Fig. 3, top right) and the derivative reflectance with fluorescence (DR*) and without fluorescence (DR) calculated (Fig. 3, middle left). The modeled fluorescence emission superimposed on the simulated reflectance with $C_{a+b}$ = 40 μg/cm$^2$ generated a double peak in the derivative reflectance when $\phi$ increased (Fig. 3, middle plot, left) due to the effect of the emission bands in the PS-I and PS-II regions. Canopy reflectance without the effects of fluorescence was simulated for different values of pigment content, and its derivative was calculated. Figure 4 shows the simulated canopy reflectance (top) and derivative reflectance (bottom) with the PROSPECT and SAILH RT models for leaf $C_{a+b}$ = 40 and 80 μg/cm$^2$, $N$ = 1.5, canopy leaf area index (LAI) = 6, plagiophile leaf angle distribution function, and nadir view. The derivative reflectance displaces toward longer wavelengths as the pigment content increases. Thus, the derivative chlorophyll index (DCI), calculated as $D_{705}/D_{722}$, is proposed here to track changes in the double peak generated by the suggested effects of CF and low $C_{a+b}$ content at the canopy level (Fig. 5). Higher values of DCI indicate the presence of such a feature.

## RESULTS

### Results of the Modeling Methods with the Fluorescence–Reflectance–Transmittance and PROSPECT Models for Chlorophyll Fluorescence and Chlorophyll *a* + *b* Estimation at the Leaf Level

Results showed that when chlorophyll content is fixed, the CUR index $[(R_{675}\cdot R_{690})/R_{683}^2]$ tracks changes in chlorophyll fluorescence. Relationships between the measured and modeled CUR were $r^2$ = 0.72 (when $\phi = F_v/F_m$), $r^2$ = 0.78 ($\phi = F'_m110$), $r^2$ = 0.5 ($\phi = \Delta F/F'_m110$), and $r^2$ = 0.34 ($\phi = \Delta F/F_m'2820$). No relationship was apparent between the measured and modeled CUR ($r^2$ = 0) when it was modeled with $\phi$ = 0, thus the coupled FRT–PROSPECT model simulates fluorescence effects accurately. Varying the emission peak center wavelength in the simulation was found to affect the relationship between the measured and modeled CUR. Better results were obtained with $F_L$ = 685 nm than with $F_L$ = 690 nm (in both cases $B_L$ = 20 nm) as indicated by $r^2$ = 0.78 ($\phi = F'_m110$; $F_L$ = 685 nm) (Fig. 6) and $r^2$ = 0.68 ($\phi = F'_m110$; $F_L$ = 690 nm). These results demonstrate that the modeled CUR performs well as a reflectance index function of fluorescence emission and that coupling PROSPECT and FRT results in an accurate simulation of the fluorescence effect in apparent reflectance. The best correlation results were obtained by selecting $F'_m110$ and $F_v/F_m$ as measures of fluorescence efficiency $\phi$, with the lack of correlation when $\phi$ = 0 demonstrating that the CUR is determined by fluorescence when $C_{a+b}$ content is constant. When both $C_{a+b}$ and CF were variable, the CUR was also affected by changes in $C_{a+b}$: $r^2$ = 0.73 when the CUR was modeled with $\phi$ = 0; $r^2$ = 0.85 ($\phi = F_v/F_m$), and $r^2$ = 0.87 ($\phi = F'_m110$). The $C_{a+b}$ estimation from the set of leaves with variable pigment content achieved $r^2$ = 0.96 and RMSE = 0.02 (Fig. 7) for comparison of estimated and measured $C_{a+b}$ concentration from each leaf. Therefore, the pigment variability within the set of leaf samples used in this study was correctly estimated with the linked FRT–PROSPECT model.

To estimate $\phi$, the coupled FRT–PROSPECT model was inverted with reflectance spectra collected in the experiments with constant and variable $C_{a+b}$ and CF. The function minimized was the RMSE between the measured and modeled CUR. Results obtained with constant $C_{a+b}$ allowed modeled fluorescence $\phi$ estimated by inversion and fluorescence variables measured with PAM (Table 1; Fig. 8) to be compared. These results

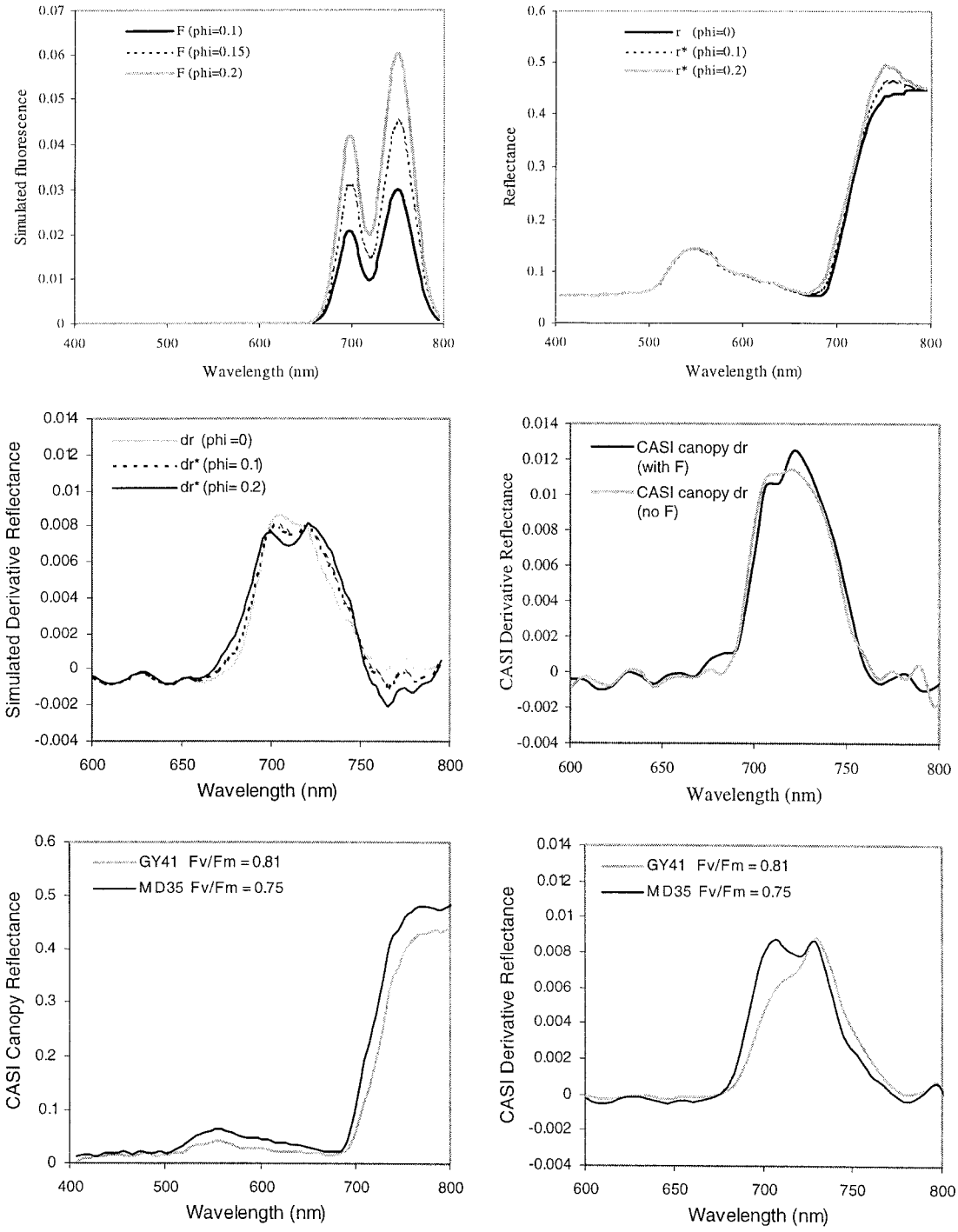


**Fig. 3. Simulated leaf reflectance including the effects of fluorescence using the fluorescence–reflectance–transmittance (FRT) model (top and middle left plots) and compact airborne spectrographic imager (CASI) reflectance in the laboratory (middle right plot) and from an airborne campaign (bottom two plots). Top left plot shows simulated fluorescence emission for different values of $\phi$ (ranging from 0 to 0.2), and superimposed on leaf reflectance (top right plot) with peaks at 695 nm ($B_L$ = 30 nm) and 750 nm ($B_H$ = 40 nm), $N$ = 1.5, and $C_{a+b}$ = 40 μg/cm$^2$. Derivative reflectance (middle left plot) for different fluorescence simulations shows a double peak as function of fluorescence emission. Laboratory CASI reflectance from sugar maple seedlings with and without fluorescence emission shows that such effects are captured on the derivative reflectance (middle right plot). Airborne CASI data collected over 30- × 30-m sugar maple study sites (bottom plots) from the two sites with highest field-measured $F_v/F_m$ and $C_{a+b}$ (GY41, $F_v/F_m$ = 0.81; $C_{a+b}$ = 38.8 μg/cm$^2$) and lowest (MD35, $F_v/F_m$ = 0.75; $C_{a+b}$ = 19.08 μg/cm$^2$) show comparable double peak features.**

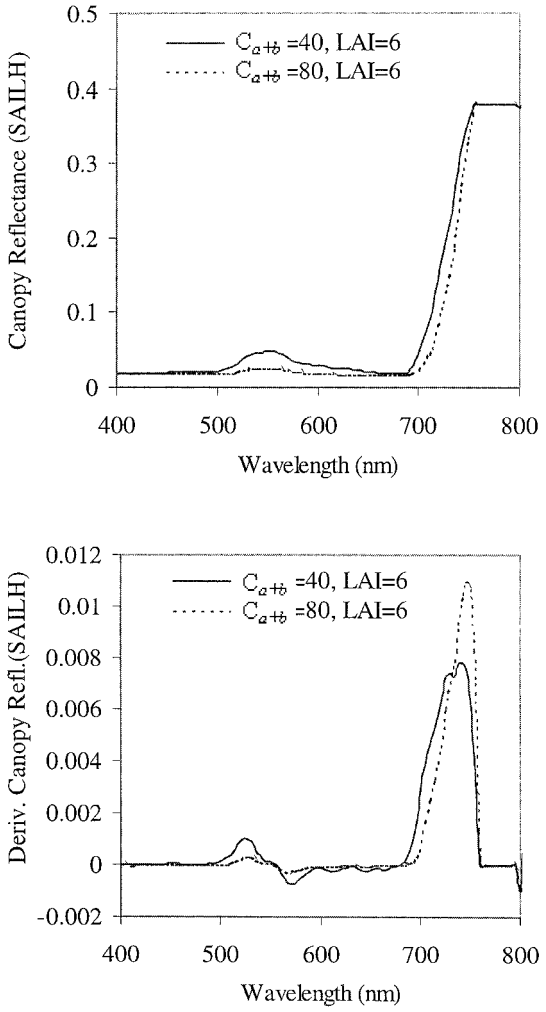


**Fig. 4. Simulated canopy reflectance (top) and derivative reflectance (bottom) using the PROSPECT and SAILH radiative transfer models for leaf $C_{a+b}$ = 40 and 80 μg/cm², $N$ = 1.5, and canopy leaf area index (LAI) = 6, plagiophile leaf angle distribution function, and nadir view.**

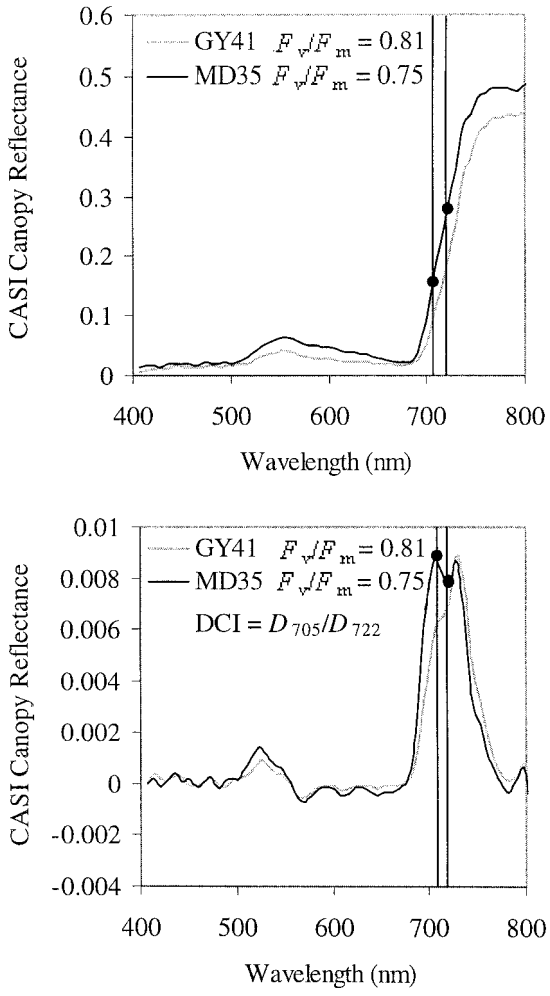


**Fig. 5. Band location of the derivative chlorophyll index (DCI) calculated as $D_{705}/D_{722}$, developed to track changes due to the double peak generated by the suggested effects of pigment and chlorophyll fluorescence at the canopy level in stressed vegetation (healthy site, GY41: $F_v/F_m$ = 0.81; $C_{a+b}$ = 38.8 μg/cm²; stressed site, MD35: $F_v/F_m$ = 0.75; $C_{a+b}$ = 19.08 μg/cm²)**

with $C_{a+b}$ constant and variable show that inversion of the coupled FRT–PROSPECT model accurately estimates ϕ, thus allowing CF to be estimated from reflectance measurements.

## Results at Canopy Level with Hyperspectral Data for Stress Detection

At the canopy level, results showed that the described double-peak effect was found on hyperspectral CASI reflectance images. Airborne imagery was analyzed from the two 20- × 20-m study areas with highest and lowest stress conditions characterized by $C_{a+b}$ and CF measured in the field. Ground-truth data from the stressed study site reported $C_{a+b}$ = 19.08 μg/cm² and $F_v/F_m$ = 0.75, while data from the healthy site resulted in $C_{a+b}$ = 38.8 μg/cm² and $F_v/F_m$ = 0.83.

Hyperspectral reflectance spectra from the healthy and stressed sites (Fig. 3, bottom left, labeled as healthy = GY41 and stressed = MD35) were used to calculate the derivative reflectance (Fig. 3, bottom right) showing the double peak suggested by the combined effects of chlorophyll fluorescence and pigment concentration on stressed vegetation. Results from the laboratory experiment with the CASI sensor collecting data from small canopies with methods for preventing induced CF emission (Fig. 3, middle, right), were consistent with results at the leaf and airborne canopy levels. The plot shows the derivative reflectance collected from the maple canopy in the laboratory with fluorescence emission (after the light source is turned on, therefore exciting fluorescence emission) and after fluorescence emission decreased. Therefore, differences in the derivative reflectance found in this experiment are due to variations in chlorophyll fluorescence tracked at the canopy level with the hyperspectral sensor in the laboratory setting.

These results suggest that hyperspectral reflectance can be used to map stress condition through optical indices calculated on the double-peak red-edge region of the derivative reflectance. The appearance of the

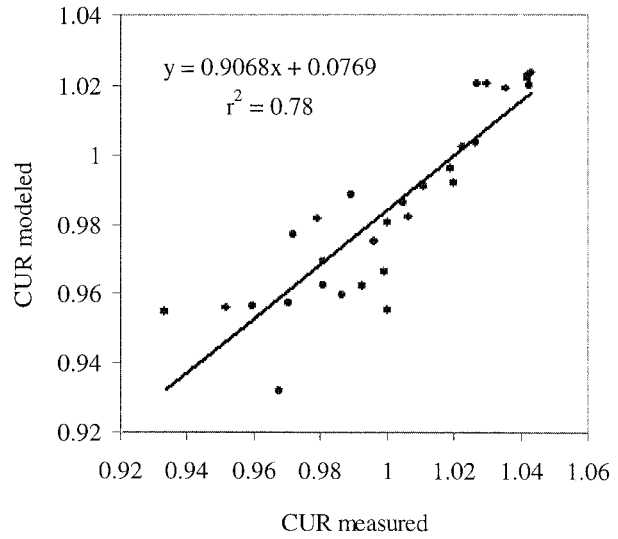


**Fig. 6. Relationship between the reflectance curvature index [CUR; $(R_{675}{\cdot}R_{690})/R_{683}^2$] measured from leaf samples (experiment with $C_{a+b}$ constant) and modeled by fluorescence–reflectance–transmittance (FRT)–PROSPECT. $F'_m110$ was used as input for $\phi$ in FRT–PROSPECT model.**

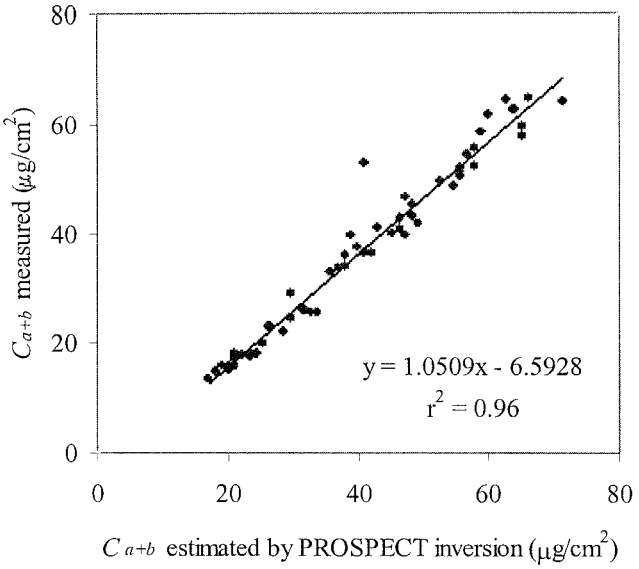


**Fig. 7. Estimation of $C_{a+b}$ by inversion of the PROSPECT leaf radiative transfer (RT) model from 60 reflectance and transmittance spectra and $C_{a+b}$ measured from leaves samples with variable chlorophyll content ($\bar{x}$ = 35.66 µg/cm², $s$ = 15.87, $n$ = 60).**

double peak could indicate stress conditions due to low pigment content and the existence of CF emission. The severity of the stress would presumably need to be significant or prolonged to exhaust the normal physiological mechanisms that quench CF (thereby reducing its emission) during early stages of stress (Mohammed et al., 1995).

The proposed DCI derivative index was applied to hyperspectral derivative reflectance collected with the CASI sensor over the two study sites with highest and lowest stress conditions (Fig. 9). The 500- × 500-m sugar maple areas showing the 20- × 20-m study sites with lowest field-measured stress (GY41, Fig. 9, top) and

**Table 1. Determination coefficients calculated between pulse amplitude modulation (PAM) chlorophyll fluorescence (CF) measurements $F_v/F_m$, $F'_m110$, $F'_m2820$, $F_t110$, $F_t2820$, $\Delta F/F'_m110$, and $\Delta F/F'_m2820$ and the estimated $\phi$ from leaf reflectance data using the fluorescence–reflectance–transmittance (FRT)–PROSPECT model.**

| | $F_v/F_m$ | $F'_m110$ | $F'_m2820$ | $F_t110$ | $F_t2820$ | $\Delta F/F'_m110$ | $\Delta F/F'_m2820$ |
|---|---|---|---|---|---|---|---|
| $C_{a+b}$ constant | 0.75 | 0.75 | 0.79 | 0.62 | 0.77 | 0.55 | 0.39 |
| $C_{a+b}$ variable | 0.5 | 0.74 | 0.66 | 0.64 | 0.62 | 0.62 | 0.33 |

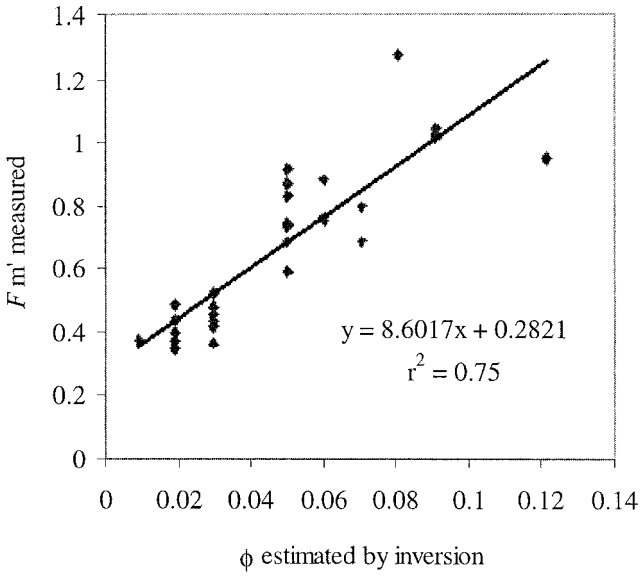


**Fig. 8. Relationship between $F'_m110$ measured from leaf samples (experiment with $C_{a+b}$ constant) and $\phi$ estimated by inversion of fluorescence–reflectance–transmittance (FRT)–PROSPECT.**

highest stress (MD35, Fig. 9, bottom) were mapped with DCI reflectance index. Areas of vegetation stress are identified on the 2- × 2-m spatial resolution airborne images in red. Results from the DCI index are consistent with the ground-truth $C_{a+b}$ and $F_v/F_m$ data measured in the field. Coefficients of determination obtained between DCI and $F_v/F_m$ ($r^2$ = 0.6) and between DCI and $C_{a+b}$ ($r^2$ = 0.42) from the airborne hyperspectral imagery collected over the 12 study sites demonstrate the relationship between ground truth measures of stress and the double-peak red-edge DCI reflectance.

## SUMMARY

Leaf-level PAM-measured fluorescence variables such as $F_v/F_m$, $F_t$, $\Delta F/F_m'$, and $F_m'$ can be estimated from leaf reflectance and transmittance by inverting the coupled FRT and PROSPECT models. Through a set of laboratory experiments with sugar maple leaves, leaf reflectance and transmittance data were collected with a LI-COR integrating sphere attached to a fiber spectrometer, as were CF measurements with a PAM fluorometer. Using the FRT model and experiments with leaf samples with constant and variable $C_{a+b}$ and CF, leaf-level optical indices that can track CF changes through measuring apparent reflectance were validated. Fluorescence-sensitive indices associated with reflectance changes at 690 and 750 nm, such as the curvature

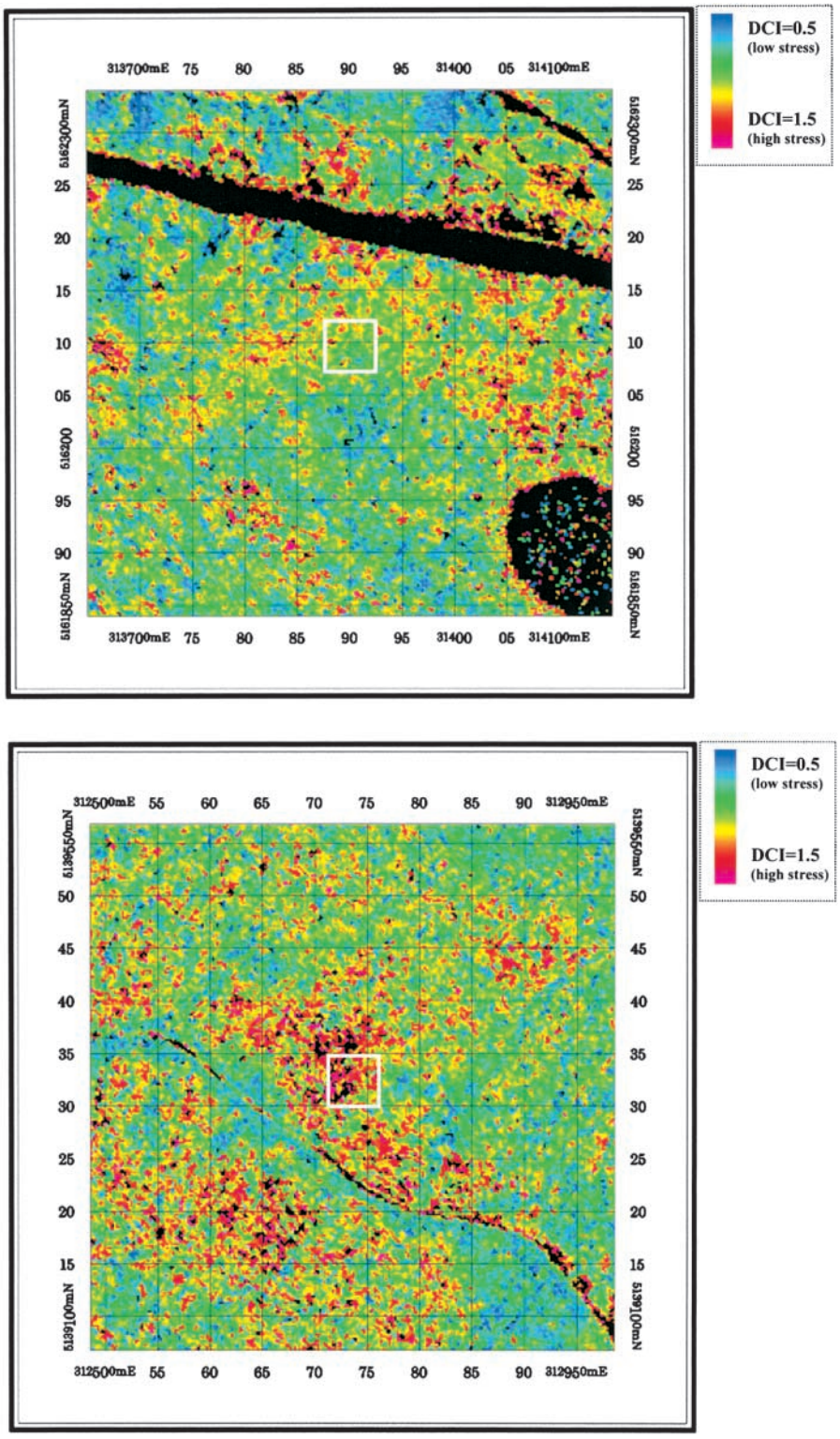


**Fig. 9. The derivative chlorophyll index (DCI) applied to hyperspectral derivative reflectance collected with the compact airborne spectrographic imager (CASI) airborne sensor. Remote sensing images were collected over the two study sites with low (top image) and high (bottom image) stress conditions to map the double peak as an indicator of stress. Images show the 500- × 500-m sugar maple areas with the 20- × 20-m study sites with highest field-measured $C_{a+b}$ and $F_v/F_m$ (GY41, $F_v/F_m$ = 0.81, $C_{a+b}$ = 38.8 μg/cm², top image) and lowest $F_v/F_m$ (MD35, $F_v/F_m$ = 0.75, $C_{a+b}$ = 19.08 μg/cm², bottom image). Areas of vegetation stress are identified on the 2- × 2-m spatial resolution airborne images in red.**

index $(R_{675} \cdot R_{690})/R_{683}^2$, were tested in numerical model inversion through FRT coupled to the PROSPECT leaf model. Inverting FRT–PROSPECT from leaf reflectance and transmittance measurements resulted in accurate estimation ($r^2 = 0.7$) of dark-adapted and steady state fluorescence measures, such as $F_v/F_m$, $F_m'$, and $F_t$. The CF and $C_{a+b}$ effects on the derivative reflectance were modeled showing a double peak in the red-edge region, which is likely due to the combined effects of fluorescence emission and low pigment content on stressed vegetation and is demonstrated by RT modeling. Consistency was found between laboratory time-decay experiments and airborne hyperspectral CASI derivative reflectance collected from two sites of extreme health conditions. The DCI calculated as $D_{705}/D_{722}$ based on the double peak of derivative reflectance is proposed for mapping vegetation stress. The coefficients of determination between the DCI calculated from 12 imaged sites of sugar maple and ground-truth $F_v/F_m$ and $C_{a+b}$ were 0.6 and 0.42, respectively. These results demonstrate the potential of derivative spectroscopy in the red-edge region with hyperspectral remote sensing to map vegetation stress effects.

#### ACKNOWLEDGMENTS

The authors gratefully acknowledge the financial support provided for this research through the Centre for Research in Earth and Space Technology (CRESTech), the Ontario Ministry of Natural Resources, and GEOIDE (Geomatics for Informed Decisions), part of the Canadian Networks of Centres of Excellence program. Special thanks are due to J. Harron (CRESTech) for developing the apparatus to perform single leaf measurements and S. Jacquemoud for making the PROSPECT code available.

## REFERENCES

Buschmann, C., and H.K. Lichtenthaler. 1988. Reflectance and chlorophyll fluorescence signatures in leaves. p. 325–332. *In* H.K. Lichtenthaler (ed.) Applications of chlorophyll fluorescence. Kluwer Academic Publ., Dordrecht, the Netherlands.

Canadian Forest Service. 1999. Forest health in Canada: An overview. Nat. Resour. Canada, Ottawa, ON.

Carter, G.A. 1994. Ratios of leaf reflectances in narrow wavebands as indicators of plant stress. Int. J. Remote Sens. 15:697–704.

Chapin, F.S. 1991. Integrated responses of plants to stress. BioScience 41:29–36.

Colombo, S.J., and W.C. Parker. 1999. Does Canadian forestry need physiology research? For. Chronicle 75:667–673.

Gamon, J.A., L. Serrano, and J.S. Surfus. 1997. The photochemical reflectance index: An optical indicator of photosynthetic radiation-use efficiency across species, functional types, and nutrient levels. Oecologia 112:492–501.

Gamon, J.A., and J.S. Surfus. 1999. Assessing leaf pigment content and activity with a reflectometer. New Phytol. 143:105–117.

Gitelson, A.A., C. Buschman, and H.K. Lichtenthaler. 1999. The chlorophyll fluorescence ratio F735/F700 as an accurate measure of chlorophyll content in plants. Remote Sens. Environ. 69:296–302.

Gitelson, A.A., and M.N. Merzlyak. 1996. Signature analysis of leaf reflectance spectra: Algorithm development for remote sensing of chlorophyll. J. Plant Physiol. 148:494–500.

Heinz-Walz-GmbH. 1993. Portable Fluorometer PAM-2000 and data acquisition software DA-2000. Heinz-Walz-GmbH, Effeltrich, Germany.

Jacquemoud, S., and F. Baret. 1990. Prospect: A model of leaf optical properties spectra. Remote Sens. Environ. 34:75–91.

Krause, G.H., and E. Weis. 1984. Chlorophyll fluorescence as a tool in plant physiology. II. Interpretation of fluorescence signals. Photosynth. Res. 5:139–157.

Larcher, W. 1994. Photosynthesis as a tool for indicating temperature stress events. p. 261–277. *In* E.D. Schulze and M.M. Caldwell (ed.) Ecophysiology of photosynthesis. Springer–Verlag, Berlin.

Lichtenthaler, H.K. 1992. The Kautsky effect: 60 years of chlorophyll fluorescence induction kinetics. Photosynthetica 27:45–55.

Lichtenthaler, H.K., and U. Rinderle. 1988. The role of chlorophyll fluorescence in the detection of stress conditions in plants. CRC Crit. Rev. Anal. Chem. 19(Suppl. 1):529–585.

Mohammed, G.H., W.D. Binder, and S.L. Gillies. 1995. Chlorophyll fluorescence: A review of its practical forestry applications and instrumentation. Scand. J. For. Res. 10:383–410.

O'Neill, N.T., F. Zagolski, M. Bergeron, A. Royer, J.R. Miller, and J. Freemantle. 1997. Atmospheric correction validation of casi images acquired over the BOREAS southern study area. Can. J. Remote Sens. 23:143–162.

Papageorgiou, G. 1975. Chlorophyll fluorescence: An intrinsic probe of photosynthesis. p. 319–371. *In* Govindjee (ed.) Bioenergetics of photosynthesis. Academic Press, New York.

Peñuelas, J., I. Filella, P. Lloret, F. Muñoz, and M. Vilajeliu. 1995. Reflectance assessment of mite effects on apple trees. Int. J. Remote Sens. 16–14:2727–2733.

Peñuelas, J., I. Filella, J. Llusia, D. Siscart, and J. Pinol. 1998. Comparative field study of spring and summer leaf gas exchange and photobiology of the mediterranean trees *Quercus ilex* and *Phillyrea latifolia*. J. Exp. Bot. 49:229–238.

Peñuelas, J., J. Llusia, J. Piñol, and I. Filella. 1997. Photochemical reflectance index and leaf photosynthetic radiation-use-efficiency assessment in Mediterranean trees. Int. J. Remote Sens. 18:2863–2868.

Rock, B.N., T. Hoshizaki, and J.R. Miller. 1988. Comparison of in situ and airborne spectral measurements of the blue shift associated with forest decline. Remote Sens. Environ. 24:109–127.

Sampson, P.H., G.H. Mohammed, P.J. Zarco-Tejada, J.R. Miller, T.L. Noland, D. Irving, P.M. Treitz, S.J. Colombo, and J. Freementle. 2000. The bioindicators of forest condition project: A physiological, remote sensing approach. For. Chronicle 76(6):941–952.

Schreiber, U., and W. Bilger. 1987. Rapid assessment of stress effects on plant leaves by chlorophyll fluorescence measurements. p. 27–53. *In* J.D. Tenhunen and E.M. Catarino (ed.) Plant response to stress. Springer–Verlag, Berlin.

Schreiber, U., W. Bilger, and C. Neubauer. 1994. Chlorophyll fluorescence as a non-destructive indicator for rapid assessment of in vivo photosynthesis. Ecol. Stud. 100:49–70.

Verhoef, W. 1984. Light scattering by leaf layers with application to canopy reflectance modeling: The SAIL model. Remote Sens. Environ. 16:125–141.

Vogelmann, J.E., B.N. Rock, and D.M. Moss. 1993. Red edge spectral measurements from sugar maple leaves. Int. J. Remote Sens. 14: 1563–1575.

Zarco-Tejada, P.J. 2000. Hyperspectral remote sensing of closed forest canopies: Estimation of chlorophyll fluorescence and pigment content. Ph.D. thesis. Graduate Program in Earth and Space Sci., York Univ., Toronto.

Zarco-Tejada, P.J., J.R. Miller, G.H. Mohammed, and T.L. Noland. 2000a. Chlorophyll fluorescence effects on vegetation apparent reflectance: I. Leaf-level measurements and model simulation. Remote Sens. Environ. 74(3):582–595.

Zarco-Tejada, P.J., J.R. Miller, G.H. Mohammed, T.L. Noland, and P.H. Sampson. 2000b. Chlorophyll fluorescence effects on vegetation apparent reflectance: II. Laboratory and airborne canopy-level measurements with hyperspectral data. Remote Sens. Environ. 74(3): 596–608.

Zarco-Tejada, P.J., J.R. Miller, G.H. Mohammed, T.L. Noland, and P.H. Sampson. 2001a. Estimation of chlorophyll fluorescence under natural illumination from hyperspectral data. Int. J. Appl. Earth Observ. Geoinfo. 3:321–327.

Zarco-Tejada, P.J., J.R. Miller, T.L. Noland, G.H. Mohammed, and P.H. Sampson. 2001b. Scaling-up and model inversion methods with narrow-band optical indices for chlorophyll content estimation in closed forest canopies with hyperspectral data. IEEE Trans. Geosci. Remote Sens. 39(7):1491–1507.